J. Chem. Soc., Faraday Trans. 1, 1988, **84**(4), 1113–1121

Ionisation Constants of $^{\bullet}OH$ and $HO_2^{\bullet}$ in Aqueous Solution up to 200 °C

A Pulse Radiolysis Study

George V. Buxton,* Nicholas D. Wood and (in part) Sally Dyster

Cookridge Radiation Research Centre, University of Leeds, Cookridge Hospital, Leeds LS16 6QB

The ionisation constant of $^{\bullet}OH$ has been determined up to 200 °C from measurements of its rate of reaction with CO_3^{2-} in alkaline solution, where $O^{\bullet-}$ is unreactive. The Van't Hoff plot shows the same curvature as that for K_w, so that $^{\bullet}OH$ and H_2O have the same heats of ionisation. ΔH for the equilibrium

$$^{\bullet}OH + OH^- \rightleftharpoons O^{\bullet-} + H_2O$$

is independent of temperature and equal to -15.4 ± 0.5 kJ mol^{-1}. ΔH for the ionisation of $HO_2^{\bullet}$ has been measured as zero within experimental error up to 175 °C by determining the concentrations of $HO_2^{\bullet}$ and $O_2^{\bullet-}$ at equilibrium from optical absorbance measurements. The activation energies for the reaction of $^{\bullet}OH$ with CO_3^{2-} and HCO_3^- are independent of temperature and equal to 23.6 ± 0.4 and 21.2 ± 0.2 kJ mol^{-1}, respectively, although $k(^{\bullet}OH + CO_3^{2-}) \approx 50\, k(^{\bullet}OH + HCO_3^-)$. The G values for e_{aq}^- and $^{\bullet}OH$ increase by 27% between 20 and 200 °C in the pH range 4.4–9.2, but appear to be independent of temperature at pH 2.

A detailed knowledge of the radiation chemistry of liquid water and aqueous solutions at elevated temperatures is necessary for accurate computer modelling of radiolytic processes in water cooled reactors. The free radicals $^{\bullet}OH$ and $HO_2^{\bullet}$ are important species in this respect and their ionisation constants are of particular interest because the dissociated forms have different reactivities from the undissociated ones.

The radiolysis of neutral water at ambient temperature is described by the reaction

$$0.42\ H_2O \rightarrow 0.28\ e_{aq}^- + 0.05\ H + 0.28\ ^{\bullet}OH + 0.04\ H_2 + 0.07\ H_2O_2 + 0.28\ H^+ \quad (1)$$

where the numbers are the yields (G values) in units of μmol J^{-1}. In the presence of oxygen reactions (2) and (3) are rapid:

$$e_{aq}^- + O_2 \rightarrow O_2^{\bullet-} \quad (2)$$

$$H + O_2 \rightarrow HO_2^{\bullet}. \quad (3)$$

The ionisation constants of $^{\bullet}OH$ and $HO_2^{\bullet}$ have been measured at *ca.* 20 °C,

$$^{\bullet}OH \rightleftharpoons O^{\bullet-} + H^+, \quad pK_4 = 11.9^1 \quad (4)$$

$$HO_2^{\bullet} \rightleftharpoons + H^+, \quad pK_5 = 4.7^2 \quad (5)$$

and their temperature dependence has been investigated over relatively short ranges.[3,4] Baxendale *et al.*[3] measured pK_4 in the range 1.6–38 °C and pK_5 in the range 3–75 °C and obtained enthalpies of ionisation of 42 ± 8 kJ mol^{-1} for $^{\bullet}OH$ and zero for $HO_2^{\bullet}$, whereas Nadezhin and Dunford[4] reported 11.3 ± 2.9 kJ mol^{-1} for $HO_2^{\bullet}$ over the range 5–25 °C.

In this paper we present information on the ionisation constants of $^{\bullet}OH$ and $HO_2^{\bullet}$ up to 200 °C.

Experimental

Solutions were made up using triply distilled water and chemicals of A.R. grade or better.

The general pulse radiolysis methods used in this laboratory have been described elsewhere.[5] In order to study aqueous solutions up to 200 °C the complete flow system was contained in a steel vessel[6] pressurised to *ca.* 2 MPa with helium. This apparatus, which was kindly loaned by Berkeley Nuclear Laboratories, CEGB, facilitates solution sample changing *in situ*. The pulse radiolysis cell was contained in a thermostatically controlled brass block and the temperature of the cell contents was measured with a thermocouple situated in a quartz sleeve which dipped into the cell.

Dosimetry was carried out at room temperature using O_2-saturated 5 mmol KI solution and measuring the absorbance due to $I_2^{\cdot-}$ at 385 nm, taking $G(I_2^{\cdot-})\varepsilon(I_2^{\cdot-}) = 3.2 \times 10^2$ m^2 J^{-1}, where $G(I_2^{\cdot-})$ is the yield of $I_2^{\cdot-}$ in μmol J^{-1} and $\varepsilon(I_2^{\cdot-})$ is the molar absorbance of $I_2^{\cdot-}$ in m^2 mol^{-1}. Corrections were made for the decrease in the density of water at elevated temperatures.

Results and Discussion

The Hydroxyl Radical

The pK of $^{\cdot}OH$ was determined by the method of Weeks and Rabani,[7] which utilises the fact that reaction (6) is fast whilst (7) is immeasurably slow:

$$^{\cdot}OH + CO_3^{2-} \rightarrow CO_3^{\cdot-} + OH^-, \quad k_6 = 4.2 \times 10^8 \text{ dm}^3 \text{ mol}^{-1} \text{ s}^{-1} \tag{6}$$

$$O^{\cdot-} + CO_3^{2-}. \tag{7}$$

Under conditions where equilibrium (8) is established;[8]

$$^{\cdot}OH + OH^- \rightleftharpoons O^{\cdot-} + H_2O, \quad k_8 = 1.3 \times 10^{10} \text{ dm}^3 \text{ mol}^{-1} \text{ s}^{-1}.[8] \tag{8}$$

the rate of formation of $CO_3^{\cdot-}$ is given by

$$\frac{d[CO_3^{\cdot-}]}{dt} = \frac{k_6[H^+]}{([H^+] + K_4)}[CO_3^{2-}][^{\cdot}OH]_T \tag{9}$$

where $[^{\cdot}OH]_T = [^{\cdot}OH] + [O^{\cdot-}]$.

In the present work solutions of carbonate were saturated with N_2O which doubles the yield of hydroxyl radicals through the reaction

$$e_{aq}^- + N_2O \rightarrow N_2 + O^{\cdot-}, \quad k_{10} = 9.1 \times 10^9 \text{ dm}^3 \text{ mol}^{-1} \text{ s}^{-1}.[9] \tag{10}$$

The solutions were subjected to a 100 ns pulse of 2.9 MeV electrons and the dose per pulse was in the range 8–11 Gy. The rate of formation of $CO_3^{\cdot-}$ was monitored by its absorbance at 600 nm and was corrected for its simultaneous decay in the reaction[10]

$$CO_3^{\cdot-} + CO_3^{\cdot-} \rightarrow CO_2 + CO_4^{2-}. \tag{11}$$

Under all conditions the kinetics of formation of $CO_3^{\cdot-}$, after applying small corrections for reaction (11), were described by

$$\frac{d[CO_3^{\cdot-}]}{dt} = k_{obs}[CO_3^{2-}]_T([CO_3^{\cdot-}]_\infty - [CO_3^{\cdot-}]) \tag{12}$$

where $[CO_3^{2-}]_T$ includes HCO_3^- formed by hydrolysis of CO_3^{2-} which can be calculated from the dissociation constant K_{13}:

$$HCO_3^- \rightleftharpoons CO_3^{2-} + H^+. \tag{13}$$

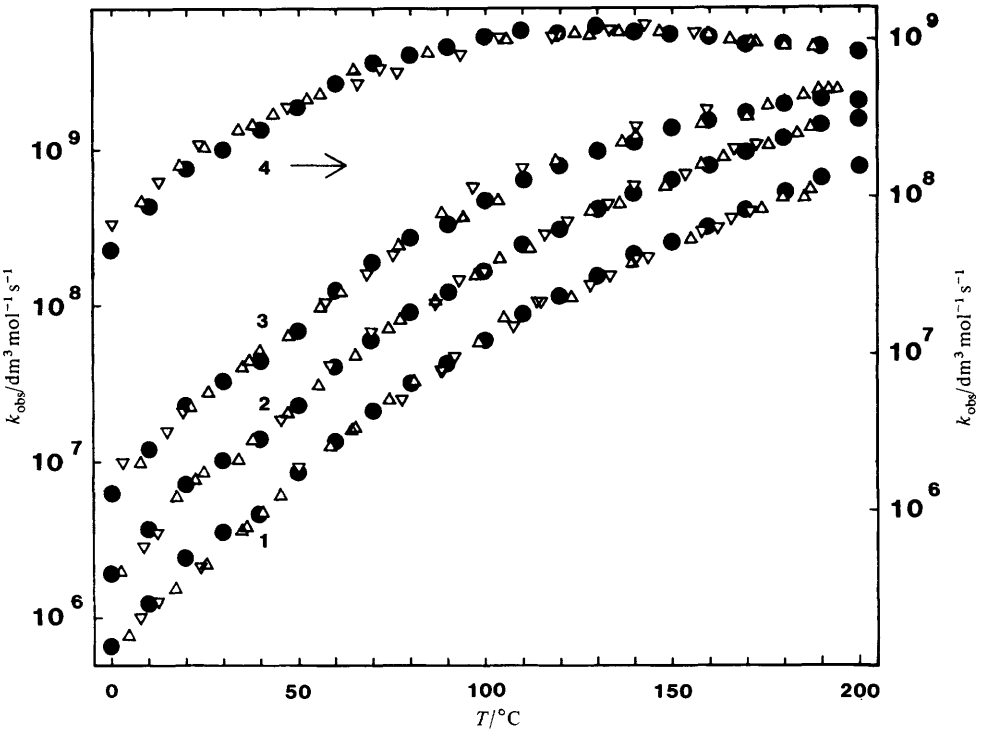

Fig. 1. Temperature dependence of k_{obs}. The data sets numbered 1 to 4 are for the following solute concentrations (mol dm^{-3}): (1) $[OH^-] = 1.0$, $[CO_3^{2-}]_T = (4\text{–}99.7) \times 10^{-2}$; (2) $[OH^-] = 0.33$, $[CO_3^{2-}]_T = (1.57\text{–}59.4) \times 10^{-2}$; (3) $[OH^-] = 0.1$, $[CO_3^{2-}]_T = (3.1\text{–}250) \times 10^{-3}$; (4) $[OH^-] = 0.01$, $[CO_3^{2-}]_T = (5.75\text{–}25.9) \times 10^{-3}$. Data are shown for increasing temperature (△), decreasing temperature (▽), and calculated from eqn (15) (●).

The total yield of $CO_3^{\cdot-}$ was equal to the total yield of $^{\cdot}OH + O^{\cdot-}$, and it was confirmed that the spectrum of $CO_3^{\cdot-}$ is independent of temperature up to 200 °C.[11]

Values of k_{obs} were measured over the range 0–200 °C for four different concentrations of hydroxide ion and a range of carbonate concentrations. The results are displayed in fig. 1 in the form k_{obs} *vs.* temperature. For clarity no more than two data points are shown for each 10 °C interval, and they comprise 20% of the total data. A feature of the data in fig. 1 is the decrease of k_{obs} at high temperature in the 10^{-2} mol dm^{-3} OH^- solution. This is attributed to the increased hydrolysis of CO_3^{2-} at high temperature and the lower reactivity of HCO_3^- with $^{\cdot}OH$:

$$^{\cdot}OH + HCO_3^- \rightarrow CO_3^{\cdot-} + H_2O, \quad k_{14} = 8.5 \times 10^6 \text{ dm}^3 \text{ mol}^{-1} \text{ s}^{-1}.[12] \qquad (14)$$

When reactions (13) and (14) are included in the mechanism k_{obs} in eqn (12) is given by

$$k_{obs} = \left(\frac{k_6}{(1 + [H^+]/K_{13})} + \frac{k_{14}}{(1 + K_{13}/[H^+])} \right) \frac{[H^+]}{([H^+] + K_4)} \qquad (15)$$

so that K_4 can be evaluated when k_6, k_{14} and K_{13} are known at the appropriate temperature

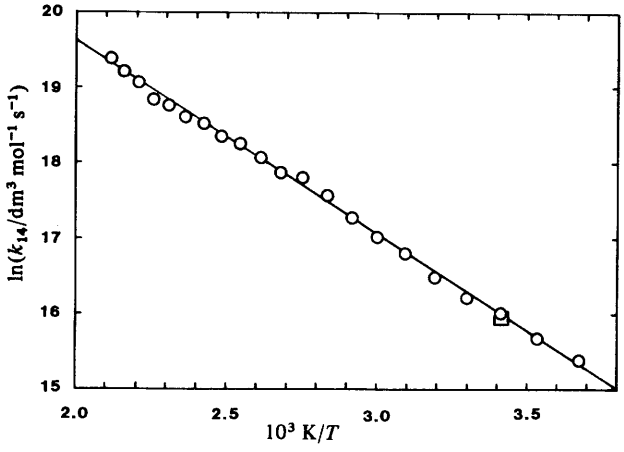

Fig. 2. Arrhenius plot for $k(\cdot OH + HCO_3^-)$. The point shown as □ is from ref. (12).

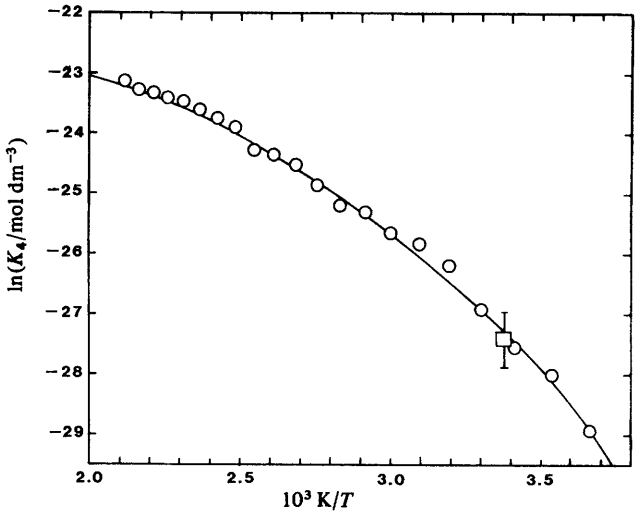

Fig. 3. Van't Hoff plot for the acid dissociation constant of ·OH. The point shown as □ is from ref. (7).

Temperature Dependence of k_{14}

When measuring k_{14} care must be taken to ensure that the bicarbonate solution is free of carbonate[12] because $K_6 = 50k_{14}$ at *ca.* 20 °C. The saturation of bicarbonate solutions with N_2O causes the pH to rise owing to the displacement of CO_2, and it is necessary to bubble CO_2 through the solution for a few seconds after N_2O-saturation to restore the pH to *ca.* 7. Values of k_{14} measured under these conditions are presented as an Arrhenius plot in fig. 2, which gives an activation energy for reaction (14) of 21.2 ± 0.2 kJ mol^{-1}. The linear Arrhenius plot in fig. 2 contrasts with the curved plot reported previously,[11] for which the HCO_3^- solutions undoubtedly contained small amounts of CO_3^{2-}. Thus the measured rate constants at low temperatures were too large, but approached the true values of k_{14} at high temperatures, where equilibrium (13) is displaced to the right.[13]

Temperature Dependence of K_4 and k_6

Values of K_4 and k_6 were calculated from the data in fig. 1 using eqn (15). K_{13} was evaluated by interpolation of a smooth curve drawn through data taken from ref. (13), and k_{14} was obtained from the linear plot in fig. 2. A trial-and-error method was then used to obtain values of K_4 and k_6 which gave good agreement between measured and calculated values of k_{obs} (see fig. 1). Their temperature dependence is shown in fig. 3 and 4, and the excellent agreement with the literature values at *ca.* 20 °C provides support for their validity.

The non-linear dependence of K_4 shows that ΔH for the ionisation of $^{\cdot}OH$ decreases with increasing temperature, as does ΔH for the ionisation of water. The temperature dependence of K_8 can be obtained from the data for K_4 and K_w;[14,15] it is described by

$$\ln K_8 = -(1.18 \pm 0.15) + (1.85 \pm 0.05) \times 10^3/T$$

which shows that ΔH for reaction (8) is independent of temperature over the range 0–200 °C and equal to -15.4 ± 0.5 kJ mol^{-1}. Baxendale *et al.*[3] obtained $\Delta H_8 = -13.8 \pm 8.4$ kJ mol^{-1} over the range 1.6–38 °C.

Note that the Arrhenius plot for k_6 is linear (fig. 4) and gives an activation energy of 23.6 ± 0.4 kJ mol^{-1} for reaction (6), which is very similar to that for reaction (14). Thus the 50-fold difference in k_6 and k_{14} occurs mainly in the Arrhenius pre-exponential factors; in terms of the collision theory, this suggests that there are more reactive encounters in the case of CO_3^{2-}. Although reaction (6) is formally written as an electron-transfer process it probably proceeds *via* addition[11] of $^{\cdot}OH$ to the C=O group because the reorganisation energy involved in forming OH^- from $^{\cdot}OH$ is rather large. The similar activation energies suggest that adduct formation also occurs with HCO_3^-, so, in view of the electrophilic nature of $^{\cdot}OH$, the difference in k_6 and k_{14} may reflect the greater resonance in CO_3^{2-}, which makes the C=O group more available compared to HCO_3^-.

The Hydroperoxyl Radical

$HO_2^{\cdot}$ was generated by pulse radiolysis of O_2-saturated 10^{-2} mol dm^{-3} formate solutions. The reactions occurring in this system are (1), (2), (3), (5), (16) and (17):

$$^{\cdot}OH + HCO_2^- \rightarrow CO_2^{\cdot-} + H_2O \quad (16)$$

$$CO_2^{\cdot-} + O_2 \rightarrow O_2^{\cdot-} + CO_2 \quad (17)$$

and conditions were chosen such that $HO_2^{\cdot}$ and $O_2^{\cdot-}$ were formed during the pulse, which was 2 μs long and delivered a dose of 40–65 Gy. In these experiments the measured quantity was $G(HO_2^{\cdot})_T\, \varepsilon_{obs}$, where $G(HO_2^{\cdot})_T$ is the sum $G(HO_2^{\cdot}) + G(O_2^{\cdot-})$ and ε_{obs} is the observed extinction coefficient. For conditions where equilibrium (5) is established, ε_{obs} is given by

$$\varepsilon_{obs} = \frac{\varepsilon(HO_2^{\cdot}) + K_5\, \varepsilon(O_2^{\cdot-})/[H^+]}{1 + K_5/[H^+]} \quad (18)$$

so that K_5 can be evaluated when $G(HO_2^{\cdot})_T$, $\varepsilon(HO_2^{\cdot})$, $\varepsilon(O_2^{\cdot-})$ and $[H^+]$ are known. The method relies on the fact that $HO_2^{\cdot}$ and $O_2^{\cdot-}$ have different spectra.[2]

The measured values of $G(HO_2^{\cdot})_T\, \varepsilon_{obs}$ are displayed in fig. 5–8. The data in fig. 5 are at pH 1.9 ($HClO_4$) where only $HO_2^{\cdot}$ is expected, and those in fig. 7 are at pH 6.8 (phosphate buffer) where only $O_2^{\cdot-}$ should be present. Similar data to those in fig. 7 were also obtained at pH 9.2 (borax buffer). The data in fig. 6 are for pH 4.4 (HCO_2H/HCO_2^-), where $HO_2^{\cdot}$ and $O_2^{\cdot-}$ are both present. Measurements at pH 1.9 and 6.8 showed that the spectra of $HO_2^{\cdot}$ and $O_2^{\cdot-}$ are independent of temperature up to 175 °C, the

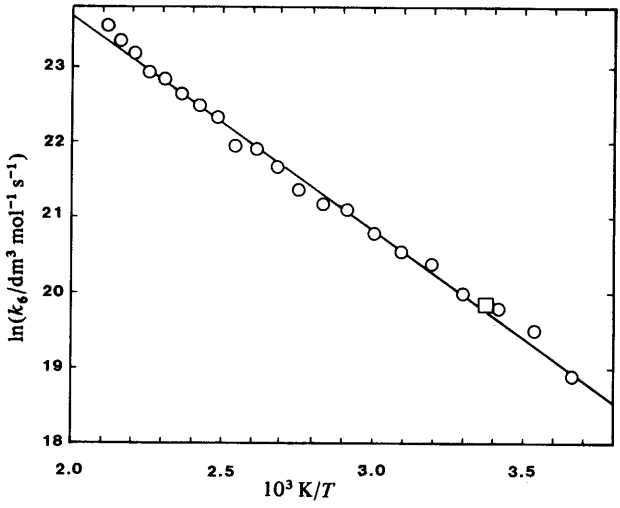

Fig. 4. Arrhenius plot from $k(\cdot OH + CO_3^{2-})$. The point shown as □ is from ref. (7).

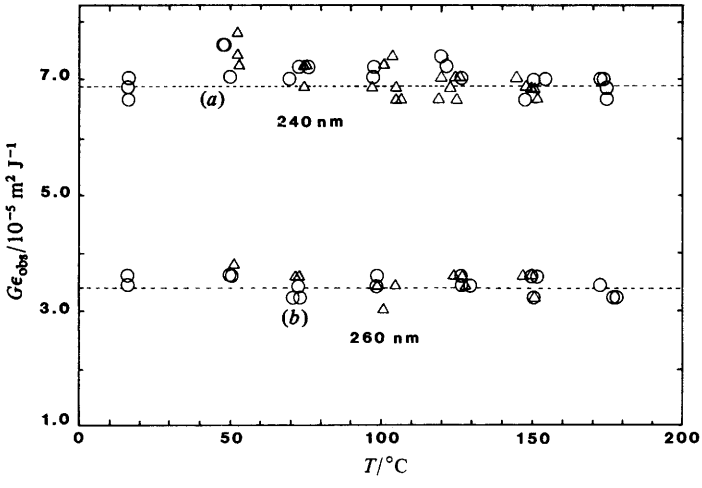

Fig. 5. Temperature dependence of $G(HO_2^{\cdot})_{T,\,obs}$ at pH 1.9: ○, increasing temperature; △, decreasing temperature. (*a*) 240 and (*b*) 260 nm.

highest temperature for these measurements. At pH 4.4, however, a small red shift was observed (see fig. 8), which points to an increase in the ratio $[O_2^{\cdot-}]$: $[HO_2^{\cdot}]$ with increasing temperature.

Evaluation of K_5 from eqn (18)

The data in fig. 5 show that $G(HO_2^{\cdot})\,\varepsilon(HO_2^{\cdot})$ is independent of temperature, whereas fig. 7 shows that $G(O_2^{\cdot-})\,\varepsilon(O_2^{\cdot-})$ increases with temperature. Since no change in the shape of the spectra of $HO_2^{\cdot-}$ or $O_2^{\cdot-}$ with increasing temperature was observed, we conclude that $\varepsilon(HO_2^{\cdot})$ and $\varepsilon(O_2^{\cdot-})$ are independent of temperature up to 175 °C. The same conclusion was reached by Baxendale *et al.*[3] up to 75 °C. It follows that $G(HO_2^{\cdot})$ at pH 1.9 is

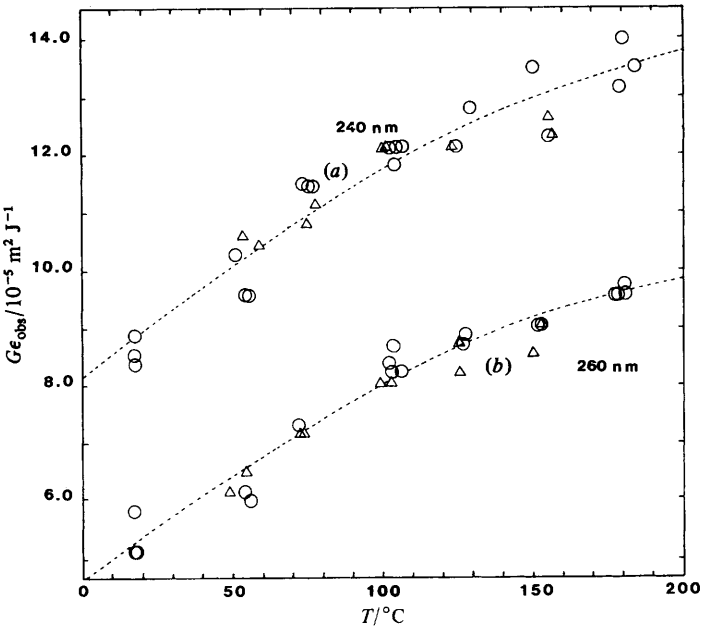

Fig. 6. Temperature dependence of $G(HO_2^{\cdot})_T \varepsilon_{obs}$ at pH 4.4: ○, increasing temperature; △, decreasing temperature. (*a*) 240 and (*b*) 260 nm.

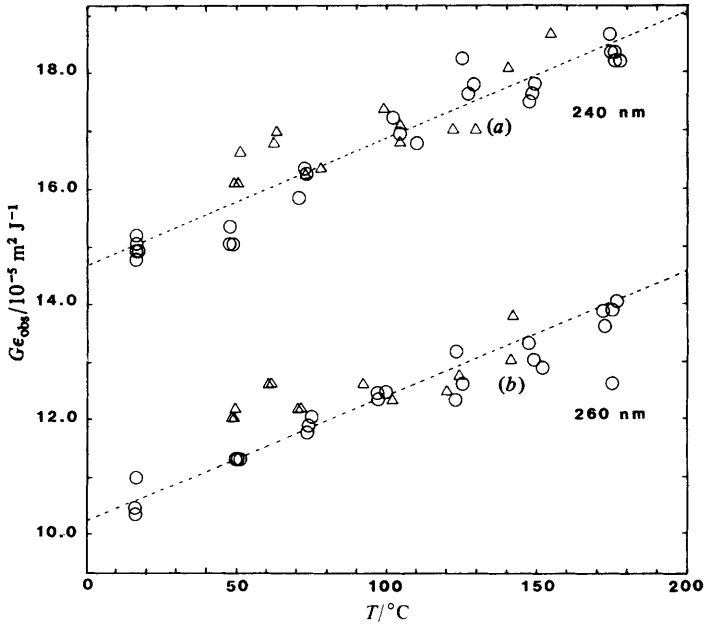

Fig. 7. Temperature dependence of $G(HO_2^{\cdot})_T \varepsilon_{obs}$ at pH 6.8: ○, increasing temperature; △, decreasing temperature. (*a*) 240 and (*b*) 260 nm.

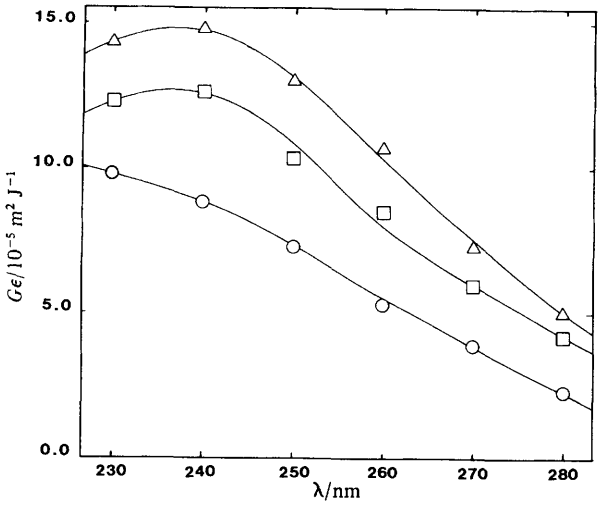

Fig. 8. Temperature dependence of the spectrum of $(HO_2^{\cdot})_T$ at pH 4.4: ○, 20; □, 100; △, 175 °C.

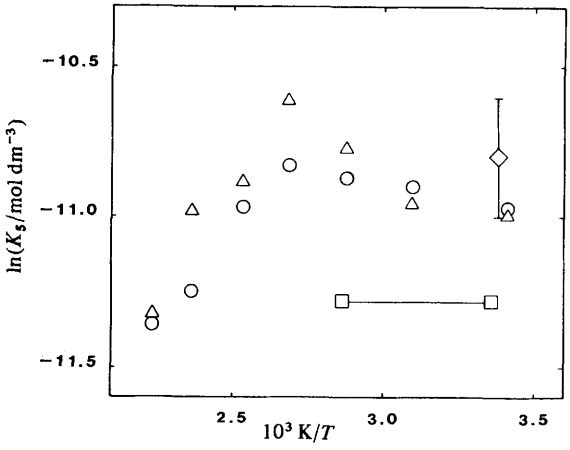

Fig. 9. Van't Hoff plot for the acid dissociation constant of $HO_2^{\cdot}$ obtained from measurements of $G(HO_2^{\cdot})_{T,\,obs}$ at 240 (○) and 260 nm (△). Also shown are data from ref. (2) (◇) and ref. (3) (□).

independent of temperature, whereas $G(O_2^{\cdot-})$ at pH 6.8 and 9.2 increases with temperature. The fractional increase in $G(O_2^{\cdot-})$ is very similar to that reported for $G(e_{aq}^-)$ over the same temperature range.[16] This is not unexpected, because $G(O_2^{\cdot-}) = G(e_{aq}^-) + G(\cdot OH) + G(H)$, $G(e_{aq}^-) + G(\cdot OH) \approx 10G(H)$ [see reaction (1)] and an increase in $G(e_{aq}^-)$ will be matched by an increase in $G(\cdot OH)$. We have also observed similar increases in N_2O-saturated solutions of bicarbonate and formate at neutral pH, which measure $G(e_{aq}^-) + G(\cdot OH)$ and $G(e_{aq}^-) + G(\cdot OH) + G(H)$, respectively.[17]

At pH 1.9 e_{aq}^- reacts with H^+ rather O_2,[18]

$$e_{aq}^- + H^+ \rightarrow H \qquad (19)$$

so the apparent lack of effect of temperature on $G(HO_2^{\bullet})$ may indicate a pH effect on spur processes in the radiolysis of water at high temperature. Further investigations in this area are planned.

At pH 4.4 the radiolysis of water [(reaction (1)] is the same at pH 6.8 and 9.2 on the timescale of the present experiments, so we assume that $G(HO_2^{\bullet})_T$ shows the same increase as $G(O_2^{\bullet-})$ at the higher pH. Therefore, in evaluating ε_{obs} from the data in fig. 6, we have divided $G(HO_2^{\bullet})_T\,\varepsilon_{obs}$ by $G(O_2^{\bullet-})$ derived from fig. 7 on the basis that $\varepsilon(O_2^{\bullet-})$ is independent of temperature. In each case the mean values indicated by the broken lines have been used. To obtain $\varepsilon(O_2^{\bullet-})$ we have taken $G(O_2^{\bullet-}) = 0.62\ \mu mol\ J^{-1}$ at 20 °C, which gives $\varepsilon(O_2^{\bullet-})$ as $172 \pm 15\ m^2\ mol^{-1}$ at 260 nm and $244 \pm 15\ m^2\ mol^{-1}$ at 240 nm; these values compare reasonably well with $193.3\ m^2\ mol^{-1}$ at 260 nm and $234\ m^2\ mol^{-1}$ at 240 nm obtained by Bielski.[2] From the data in fig. 5 and taking $G(HO_2^{\bullet}) = 0.62\ \mu mol\ J^{-1}$ we obtain $\varepsilon(HO_2^{\bullet}) = 57 \pm 3$ and $110 \pm 7\ m^2\ mol^{-1}$ at 260 and 240 nm, respectively, compared with Bielski's values of 54.3 and $126.2\ m^2\ mol^{-1}$.[2]

Fig. 9 shows a Van't Hoff plot of K_5, where the values of K_5 have been determined using our measured values of $\varepsilon(HO_2^{\bullet})$ and $\varepsilon(O_2^{\bullet-})$ and allowing for the change in the dissociation constant of formic acid with temperature.[19] Within the uncertainty of the experimental data ΔH_5 is zero up to 175 °C. Thus the present work confirms the findings of Baxendale *et al.*,[3] but over a much wider range of temperature.

Finally, the constancy of K_5 and linearity of the Van't Hoff plot for K_8 provide a firm basis for extrapolation of these data to higher temperature.

We are grateful to AERE, Harwell for financial support and to C.E.G.B., Berkeley Nuclear Laboratories for the loan of the high-temperature apparatus.

References

1 J. Rabani and M. S. Matheson, *J. Am. Chem. Soc.*, 1964, **86**, 3175.
2 B. J. H. Bielski, *Photochem. Photobiol.*, 1978, **28**, 645.
3 J. H. Baxendale, M. D. Ward and P. Wardman, *Trans. Faraday Soc.*, 1971, **67**, 2532.
4 A. Nadezhdin and H. B. Dunford, *J. Phys. Chem.*, 1979, **83**, 1957.
5 D. H. Ellison, G. A. Salmon and F. Wilkinson, *Proc. R. Soc. London, Ser. A*, 1972, **328**, 23.
6 R. Rist, *Ph.D. Thesis* (University of Nottingham, 1983).
7 J. L. Weeks and J. Rabani, *J. Phys. Chem.*, 1966, **70**, 2100.
8 G. V. Buxton, *Trans. Faraday Soc.*, 1970, **66**, 1656.
9 R. H. Schuler, A. L. Hartzell and B. Behar, *J. Phys. Chem.*, 1981, **85**, 192.
10 J. Lilie, A. Henglein and R. J. Hanrahan, *Radiat. Phys. Chem.*, 1978, **17**, 3157.
11 D. R. McCracken and G. V. Buxton, *Nature (London)*, 1981, **292**, 439.
12 A. J. Elliot and G. V. Buxton, *Radiat. Phys. Chem.*, 1986, **27**, 241.
13 *Stability Constants* (Special Publication of the Chemical Society no. 25, 1971).
14 *Handbook of Physics and Chemistry*, 55th edn, (CRC Press, Boca Raton, FL, 55th edn., 1975).
15 G. J. Bignold, A. D. Brewer and B. Hearn, *Trans. Faraday Soc.*, 1971, **67**, 2419.
16 K. N. Jha, T. G. Ryan and G. R. Freeman, *J. Phys. Chem.*, 1975, **79**, 868.
17 G. V. Buxton and N. D. Wood, to be published.
18 M. Anbar, M. Bambenek and A. B. Ross, *Natl. Stand. Ref. Data Ser., Natl. Bur. Stand. (U.S.)* 1973, **43**.
19 G. J. Bignold and R. J. Bawden, Central Electricity Research Laboratories, Leatherhead, Laboratory Note no. RD/L/N169/73, 1973.

Paper 7/779; *Received* 1st *May*, 1987